

1 **A Comparison of Machine Learning Methods 2 for Predicting the Compressive Strength of Field-Placed Concrete**

3 *M.A. DeRousseau¹, E. Laftchiev², J.R. Kasprzyk¹, B. Rajagopalan¹, W.V. Srubar III^{1,†}*

4 ¹Department of Civil, Environmental, and Architectural Engineering, University of Colorado Boulder,
5 ECOT 441 UCB 428, Boulder, Colorado 80309-0428 USA,

6 ²Mitsubishi Electric Research Labs, 201 Broadway FL8, Cambridge, MA 02139

7 [†]Corresponding Author, T +1 303 492 2621, F +1 303 492 7317, E wsrubar@colorado.edu

9 **Abstract**

10 This study evaluates the efficacy of machine learning (ML) methods to predict the compressive strength
11 of field-placed concrete. We employ both field- and laboratory-obtained data to train and test ML models
12 of increasing complexity to determine the best-performing model specific to field-placed concrete. The
13 ability of ML models trained on laboratory data to predict the compressive strength of field-placed
14 concrete is evaluated and compared to those models trained exclusively on field-acquired data. Results
15 substantiate that the random forest ML model trained on field-acquired data exhibits the best performance
16 for predicting the compressive strength of field-placed concrete; the RMSE, MAE, and R² values
17 were 730 psi, 530 psi, and .51, respectively. We also show that hybridization of field- and laboratory-
18 acquired data for training ML models is a promising method for reducing common over-prediction issues
19 encountered by laboratory-trained models that are used in isolation to predict the compressive strength of
20 field-placed concrete.

21
22 **Keywords:** concrete; compressive strength; machine learning; prediction; statistical modeling

24 **1. Introduction**

25 The 28-day compressive strength of concrete is a critical design parameter for reinforced concrete
26 structures [1]. Empirical prescriptive- and performance-based mixture design methodologies remain the
27 conventional means to obtain concrete mixture design proportions that meet minimum 28-day
28 compressive strength requirements. However, numerical approaches for predicting the 28-day
29 compressive strength of concrete are emerging in the literature. Accurate numerical estimation of the 28-
30 day compressive strength of concrete is desirable because more precise prediction (1) provides assurance
31 of concrete quality, (2) reduces the number of concrete batches that are needed to be tested to meet
32 strength targets, and (3) enables a reduction in factors of safety. Recent computational studies have
33 demonstrated the ability of advanced statistical modeling techniques to numerically predict concrete
34 compressive strength for laboratory-mixed concrete, termed *laboratory concrete* herein [2]–[13].

35 However, prediction of the 28-day compressive strength of concrete placed in the field on an actual
36 construction site, termed *field concrete* herein, remains a challenge for the concrete industry due to
37 variable environmental conditions and other uncertainties encountered during mixture proportioning,
38 transport, placing, curing, and finishing.

39 *1.1 Prediction challenges for field concrete mixtures*

40 Estimating the 28-day compressive strength of concrete is a multifaceted problem. Complex physical and
41 chemical interactions occur between concrete constituents, which, in turn, affect compressive strength.
42 Therefore, nonlinear mathematical models are advantageous for accurately capturing all phenomena. As
43 an example, consider the following physically intuitive correlations: compressive strength decreases
44 (nonlinearly) as the water-to-cement ratio (w/c) increases [14], [15]; increasing air content for improved
45 workability and freeze-thaw resistance also reduces compressive strength [16]. Other correlations have
46 not been as intuitively deduced to-date. For example, it is well known that the proportion of coarse-to-fine
47 aggregate affects compressive strength, but the relationship has not been precisely determined due to
48 confounding factors, such as particle size distribution, aggregate angularity, and water demand. Coarse
49 aggregate, for example, may vary in nominal size, grading, chemical composition, shape, surface texture,
50 and absorptivity [17]; these properties can impact the strength of the interfacial bonds between the
51 aggregate and mortar, which, in turn, affect the compressive strength of concrete. Furthermore, the
52 addition of supplementary cementitious materials (SCMs), like fly ash, slag, and silica fume, also
53 introduce new, complex, and nonlinear relationships to compressive strength because of complex factors,
54 such as fineness, chemical variability, and pozzolanic reactivity [18], [19]. Additionally, the fineness and
55 mineral composition of fly ash and slag can be highly variable, depending on the original industrial
56 source and additional processing steps [20].

57 The conditions of the job site at which field concrete is mixed and placed are also highly variable and
58 lead to high variability in field compressive strength compared to laboratory concrete. For instance, it is
59 commonplace for the environmental conditions at construction sites to be loosely controlled. Here,
60 temperature, humidity, and inclement weather can all affect concrete curing and the final compressive
61 strength [21], [22]. Such variabilities do not exist in laboratory concrete mixing, which suggests that
62 accurate prediction of the compressive strength of field concrete is a more challenging problem compared
63 to compressive strength prediction of laboratory concrete.

64 *1.2 Machine learning methods for compressive strength prediction*

65 Because of the physical limitations described above, there is growing interest in predicting concrete
66 compressive strength using machine learning (ML) models for both field and laboratory concrete
67 mixtures [23], [24]. ML models predict compressive strength (*i.e.*, the target variable) from the types and
68 quantities of the mixture ingredients (*i.e.*, the input variables). Using pairs of data of the form [input

69 variables, target variable], a model is trained from a collected dataset and learns the relationship between
70 the target and input variables without constraint on prior intuitive understanding. The vast majority of this
71 type of research has been performed on laboratory concrete, which, as discussed, suggests limitations on
72 the actual usefulness of these models for predicting the compressive strength of field concrete, given the
73 myriad of convoluting factors.

74 Prior research in ML methods for compressive strength prediction has been limited to testing ML
75 methods using laboratory data to determine best-possible prediction models for concrete compressive
76 strength. A particularly popular ML algorithm is artificial neural networks (ANNs). The first study of
77 ANNs by Yeh *et al.* [25] employed ANNs on a dataset of over 1000 laboratory concrete mixture designs.
78 Since then, other researchers have reported ANN studies with coefficients of determination (R^2) of up to
79 0.999 [2]–[8], [10], [26]–[28]. However, a significant number of ANN studies employ less than 100
80 experimental data points, which may not sufficiently sample the predictor variable space. While ANNs
81 are a flexible and powerful ML method, it suffers from the need to train a large number of parameters.
82 For small datasets (as is common for field concrete), ANNs can quickly overfit the data, which leads to
83 strong training set performance but poor generalization performance on new datasets. Other ML methods
84 that appear in the literature include support vector machines (SVM) [25], [26] and decision tree-based
85 models [13], [29]. Studies that employ these methods are less common than ANN studies, due to the
86 historical alignment of compressive strength prediction and ML methods.

87 Some narrower-scope prediction studies that used ML have focused on modeling concrete mixtures
88 that contain particular mixture ingredients, such as fly ash [28], blast-furnace slag [30], recycled
89 aggregate [31], silica fume [32], and metakaolin [33]. This body of research generates models that are
90 useful for predicting compressive strength when specific constituents are included. However, this
91 approach narrowly tailors the model to the particular dataset and, thus, is less useful when either mixture
92 ingredients or external conditions (possibly unmeasured) may change.

93 A recent study by Young *et al.* considered field concrete data and compared the predictive
94 performance of four ML models for predicting both *field* and *laboratory concrete* [23]. This study found
95 that variance can be significantly better explained in the laboratory concrete dataset, which is compatible
96 with the idea that *laboratory concrete* has fewer uncontrolled variables. The study determined that the
97 four ML methods investigated exhibited equivalent predictive performance for *field concrete* – a
98 somewhat unintuitive result, given that the four methods employed do not share common assumptions
99 about the underlying data. In addition, it is also of note that the laboratory and field datasets contained
100 different mixture ingredients (*i.e.*, input variables). For example, the laboratory concrete dataset included
101 blast-furnace slag, while the field concrete dataset did not, making an apples-to-apples comparison
102 difficult between models for both laboratory and field concrete.

103 *1.3. Innovative contribution/knowledge gaps*

104 Despite a large body of research in this area of study, the challenge of training a ML model for accurate
105 prediction of concrete compressive strength remains relevant. More specifically, two significant gaps
106 exist in the literature. First, prior studies are not well-grounded in best-practice methods of the ML
107 community. The standard procedure in ML is to generate a pipeline of methods that increase in
108 complexity [34]. The reason for this is two-fold: (1) while powerful, ML methods often search a large
109 model space and may miss simple solutions recognized by the researcher and (2) the failure of simpler
110 models is typically caused by a failure in model assumptions that reveals previously hidden details about
111 the data interactions and non-linear behavior observed in the system. These failures can thus be used to
112 inform the appropriate choice of ML tools for further development. Second, consensus on the best model
113 architectures for predicting the compressive strength of field concrete has not yet been reached.

114 To this end, this study aims to address the aforementioned knowledge gaps and is particularly focused
115 on approaches for accurate prediction of the compressive strength of *field concrete*. First, we employ the
116 standard ML procedure of testing models of increasing complexity in order to determine the best-
117 performing model for field concrete. This procedure enables us to build on past research by discussing
118 *why* certain ML methods are particularly well-suited for the concrete compressive strength prediction
119 problem. The field concrete dataset in this study contains 1681 concrete mixtures and was collected by
120 the Colorado Department of Transportation (CDOT). The laboratory concrete dataset in this study was
121 obtained from the University of California, Irvine Machine Learning Repository, which contains data for
122 more than 1000 mixtures [35].

123 Following the analysis of the field concrete models trained on the field concrete dataset, we evaluate
124 the ability of ML models learned on laboratory concrete data to predict the compressive strength of field
125 concrete mixtures. For this analysis, we perform the same ML procedures for the laboratory data and
126 select the best-performing model. This model is then used to predict the compressive strength of field
127 concrete mixtures, and the relative model performance is analyzed. It was hypothesized that the
128 laboratory ML model performance would be unsatisfactory for predicting field compressive strength
129 compared to that of models trained exclusively on field concrete data. Finally, this work includes an
130 analysis of laboratory data-trained models that are supplemented with varying percentages of field data in
131 order to determine if such hybridized datasets can improve performance the predictive capabilities of
132 laboratory concrete models.

133 **2. Machine Learning (ML) Methods**

134 As discussed in the introduction, this paper builds a pipeline of ML methods with increasing complexity,
135 such that the underlying structure in the training data can be stepwise analyzed. First, in Section 2.1, we
136 describe the ML methods used in the pipeline. We introduce *linear methods* (*i.e.*, linear regression,

137 polynomial regression), *transformed linear methods* (i.e., kernelized support vector regression, kernelized
 138 Gaussian process regression), and *non-linear methods* (i.e., regression trees, boosted trees, random
 139 forest). In general, simple models are introduced first, and subsequent models increase in complexity. The
 140 simplest methods (e.g., linear regression) tend to require the most assumptions about the underlying data
 141 structure, and the most complex methods (e.g., boosted trees) require few assumptions about the
 142 underlying structure of the data. Second in Section 2.2, we analyze the utility of predictive models trained
 143 on laboratory concrete data for predicting field concrete strength. Third, in Section 2.3, we introduce the
 144 performance measures used to evaluate the effectiveness of each model: the coefficient of determination
 145 (R^2), root mean squared error (RMSE), and mean absolute error (MAE). Last, in Section 2.4, overfitting is
 146 discussed, which occurs when a model not only captures the desired qualities in the data, but also begins
 147 to exactly model the training data itself. An overfitted model is undesirable because it lowers the
 148 predictive performance on “unseen” testing data. In other words, overfitted models do not generalize well
 149 to real-world cases. In this analysis, we describe and utilize nested cross-validation as a means reduce
 150 overfitting. Reserved testing data is used for final determination of the best-performing model.

151 **2.1 ML Methods**

152 All models were created in the R Project for Statistical Computing [36]; in addition, Table 1 lists the ML
 153 methods employed in this study, as well as the specific package and function used for model training. For
 154 each ML method, we discuss parameter tuning and the intuitive meaning of the parameters.

155 **Table 1.** ML models and corresponding R packages used in this study.

Model Type	R Package	R Function
<i>Linear Methods</i>		
Linear regression	stats	lm
Polynomial regression	stats	lm
<i>Transformed Linear Methods</i>		
Kernelized support vector regression	kernlab	ksvm
Kernelized Gaussian process	kernlab	gausspr
<i>Non-Linear Methods</i>		
Regression trees	rpart	rpart
Random forest	randomForest	randomForest
Boosted trees	gbm	gbm

156

157 **2.1.1 Linear Regression**

158 The simplest model to apply and analyze is linear regression. In addition to providing useful
 159 understanding of the data, linear regression also serves as a good baseline from which other techniques
 160 can be evaluated. Linear regression is a model that describes the output (target) variable as a linear
 161 combination of the predictor variables [37]. This linear combination is a hyperplane in N-dimensional
 162 space, where N is the number of coefficients in the model. The model solution is the hyperplane that

163 minimizes the squared error between the observed output and the predicted output. Mathematically, the
164 solution is described as:

165
$$\hat{y} = \mathbf{x}^T \boldsymbol{\beta}, \quad \text{Eq. 1}$$

166 where \mathbf{x} is the input vector, $\boldsymbol{\beta}$ is the N-dimensional vector of coefficients (parameters) for the linear
167 model, and \hat{y} is the predicted output variable from the model. The underlying assumption in linear
168 regression is that the relationship between the predictor variables and the output variable is linear.
169 Moreover, the model assumes that predictor variables are independent from one another, and the resulting
170 residuals, the difference between the predicted and observed output variables, are both homoscedastic
171 (i.e., have constant variance) and normally distributed. When these assumptions are violated, it indicates
172 that a linear model is not appropriate. When such violations occur, it is reasonable to use transformations
173 on the input data to try to reduce or eliminate the violation in assumptions. Failure of such methods to
174 improve the resulting model error and reduce violation of the assumptions means that the dataset requires
175 more complex non-linear models.

176 **2.1.2 Multivariate Polynomial Regression**

177 Multivariate polynomial regression (called *polynomial regression* in this study) uses nth degree
178 polynomials of the input variables to predict the output variable. Polynomial regression is a generalization
179 of Eq. 1; however, each x term may be: (1) an original predictor variable (e.g., x_1), (2) a pure higher-order
180 term of one predictor variable (e.g., x_1^4), or (3) an interaction term between two or more predictor
181 variables (e.g., $x_1x_2^2$)

182 A generalized example of an expanded second-order polynomial solution with two predictor variables
183 (for simplicity) is described by:

184
$$\hat{y} = \beta_0 + \beta_1 x_1 + \beta_2 x_2 + \beta_{11} x_1^2 + \beta_{22} x_2^2 + \beta_{12} x_1 x_2 \quad \text{Eq. 2}$$

185 The transformation of the predictor variables allows for modeling of higher-order relationships and
186 modeling interactions between the input variables; Eq. 2, for example, shows a parabolic relationship.
187 When the original predictor variables are transformed, they are called “features.” This term, also
188 commonly applied to all input variables of the models, denotes the fact that the inputs have been
189 transformed from their original space. In this analysis, polynomials up to third-order are employed, where
190 third order is chosen due to limits in computational power. Since polynomial regression is a form of linear
191 regression, the same assumptions are required—more specifically, independence of the input features,
192 homoscedasticity of the residuals, and normality of the residuals. Note, however, these assumptions apply
193 to the transformed features and not the original data space.

194 **2.1.3 Kernalized Regression Methods**

195 Kernalized regression methods utilize two mathematical concepts applied in tandem – a transformation of
 196 the predictor variables and the pairing of the new predictors with a regression method. These pairings can
 197 then be analyzed in order to determine which (if any) kernel and regression assumptions fit the data well.

198 Kernels are a set of transformations that can be used to map the original predictor variable space to a
 199 high-dimensional feature space [34]. Here, this mapping is more complex than the polynomial mappings
 200 in the previous section, and all mappings are the result of extensive previous research effort [38]. Each
 201 kernel has its own set of *tuning parameters* that must be optimized. This paper compares four kernel
 202 transformations, including: linear kernel, radial basis function (RBF) kernel, sigmoid kernel, and
 203 polynomial kernels (up to order 4). The model order of the polynomial kernels is only limited by the
 204 available computational power.

205 Kernel transformations have the form:

$$206 \quad k(\mathbf{x}, \mathbf{x}') = \langle \phi(\mathbf{x}), \phi(\mathbf{x}') \rangle \quad \text{Eq. 3}$$

207 where k is the kernel function, \mathbf{x} and \mathbf{x}' are N -dimensional input vectors (N is the number of predictor
 208 variables), and ϕ is a mapping from m dimensions to an m -dimensional space. Note that $\langle \phi(\mathbf{x}), \phi(\mathbf{x}') \rangle$
 209 denotes the inner product between the two mappings and can be thought of as a measure of similarity
 210 between the two transformed vectors. The kernel tuning parameters are optimized in tandem with the
 211 optimization of a regression model. This optimization is discussed below. Table 2 provides the kernel
 212 transformation equations and kernel tuning parameters used in this study.

213 **Table 2.** Kernel Transformation equations and tuning parameters

Name	Kernel Transformation	Tuning Parameters
Linear	$k(\mathbf{x}, \mathbf{x}') = \langle \mathbf{x}, \mathbf{x}' \rangle$	n/a
Radial Basis Function	$k(\mathbf{x}, \mathbf{x}') = \exp(-\gamma \ \mathbf{x} - \mathbf{x}'\ ^2)$	γ
Polynomial	$k(\mathbf{x}, \mathbf{x}') = (\gamma \langle \mathbf{x}, \mathbf{x}' \rangle + r)^d$	γ , r , and d

214
 215 The transformed variables (features) can be utilized with any regression method. The concept here is that
 216 parameters for both the kernel transformations and the regression methods are tuned simultaneously such
 217 that the cross-validated model error is minimized. When there are multiple tuning parameters, a grid
 218 search technique is employed in order to find near-optimal parameter values. In this paper, two kernalized
 219 regression methods are tested: support vector regression and Gaussian process regression.

220 Support vector regression (SVR) is a version of support vector machines (SVM) used for regression
 221 purposes (rather than classification) [39]. The regression model generated by SVR depends on only a
 222 subset of the dataset, and these data points are deemed *support vectors*. When an SVR model is trained,
 223 support vectors are the points from the dataset that produce error values (ϵ) larger than a prescribed

224 threshold value. SVR model training generates values for β_m (the coefficients for the transformed support
 225 vectors) and β_0 (the intercept). This occurs via minimization of Eq. 4 using gradient descent:

$$226 \quad \min: H(\beta_m, \beta_0) = \sum_{i=1}^N V(y_i - \hat{y}) + \frac{\lambda}{2} \sum \beta_m^2 \quad \text{Eq. 4}$$

227 Here, $V(r)$ is the prescribed error measure, y is the observed target variable, and λ is a regularization
 228 parameter that serves as a degree of importance given to large error values. When λ increases, large errors
 229 are more greatly penalized in the model; this parameter can be tuned using cross-validation. In this study
 230 the SVR is paired with the aforementioned kernel transformations in order to examine the utility of
 231 transformations of the predictor variables.

232 The second regression method that is employed with the kernel-transformed data is Gaussian process
 233 regression (GP). GP can be thought of as the Bayesian interpretation of linear regression. Rather than
 234 assuming that the relationship between the predictor variables and the target variable has the prescribed
 235 linear functional form (e.g. $\hat{y} = \mathbf{x}^T \boldsymbol{\beta}$), GP simply assumes that the data can be represented as a sample
 236 from a multivariate Gaussian distribution and that the mean of this distribution is zero. This approach is
 237 “less parametric” in the sense that the model is more loosely defined. Using GP, the predictions of the
 238 target variable are made using the conditional probability, $p(y_* | \mathbf{y})$. In short: given the data, how likely is
 239 a certain prediction for y_* ? Here, note the subtle difference between \hat{y} and y_* . \hat{y} represents a predicted
 240 target variable from a model, and y_* represents a distribution of possible outputs from the model. In the
 241 case of GP, \hat{y} is the expected value of y_* , $E[y_*] = E[y_* | \mathbf{y}]$.

242 Given the assumed Gaussian distribution, the matrix of all predictor variables in the dataset (\mathbf{X}), the
 243 output vector (\mathbf{y}) and the new matrix of data inputs, the goal is to make a prediction on the new set of data
 244 points (\mathbf{x}_*). The derived conditional distribution has the form,

$$245 \quad y^* | \mathbf{y} \sim N(\mathbf{K}_* \mathbf{K}^{-1} \mathbf{y}, \mathbf{K}_{**} - \mathbf{K}_* \mathbf{K}^{-1} \mathbf{K}_*^T), \quad \text{Eq. 5}$$

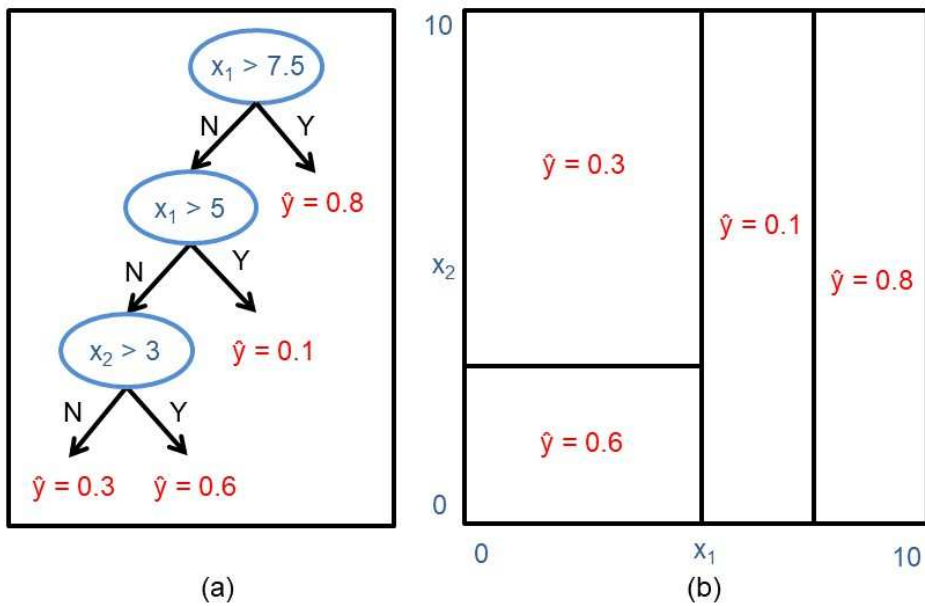
246 where \mathbf{K} , \mathbf{K}_* , and \mathbf{K}_{**} are the covariance matrices resulting from $k(\mathbf{x}, \mathbf{x}')$, $k(\mathbf{x}_*, \mathbf{x}')$, and $k(\mathbf{x}_*, \mathbf{x}_*')$,
 247 respectively. The prediction, \hat{y} , is the expected value of this distribution, which can be reduced to the
 248 equation below.

$$249 \quad \hat{y} = \mathbf{K}_* \mathbf{K}^{-1} \mathbf{y} \quad \text{Eq. 6}$$

250 Since GP employs only the assumption of a Gaussian distribution and the covariance matrices for model
 251 formulation, no tuning parameters are necessary for this regression method beyond those required for the
 252 choice of kernel. The performance of GP allows us to assess the veracity of the Gaussian distribution
 253 assumption for the data under multiple different transformations of the predictor variables. If none of the
 254 above regression methods can adequately model the output variable, models with no linearity assumptions
 255 (e.g. regression trees, artificial neural networks) are reasonable model options consider.

256 **2.1.4 Regression Trees**

257 The goal of a regression tree is to generate partitions in the predictor variables such that the target variable
 258 can be predicted based on the partitions among the input variables. Figure 1a provides a simple
 259 illustration of regression tree “nodes” (*i.e.*, partition rules) and “leaves” (*i.e.*, terminal nodes that lead to
 260 one output value). For instance, in the example provided in Figure 1a, there are two predictor variables (x_1
 261 and x_2). The “root node” (the uppermost blue ellipse) is a rule that partitions the data along x_1 . For this
 262 node, if x_1 is greater than 7.5, then the predicted output (in red) is 0.8. However, if the value of x_1 is less
 263 than 7.5, then one must proceed to the next node in the tree. This process continues until a predicted
 264 output variable is reached. For the same example regression tree, Figure 1b demonstrates that a regression
 265 tree partitions the predictor variables into rectangular spaces; the and the predicted output is the same
 266 value throughout each of these rectangular cells.



267

268 **Figure 1:** (a) Diagram of an example regression tree model with two predictor variables, x_1 and x_2 . (b)
 269 This diagram shows the same decision tree using the two predictor variables as axes. It helps visualized
 270 the rectangularity of the target variable predictions when simple regression trees are employed. Within
 271 each rectangle the predicted target variable would be the same.

272 Training a regression tree is performed by selecting partitions in succession using a criterion of
 273 variance reduction in the target variable [40]. Since each successive partition is always chosen such that
 274 the variance of the target variable is reduced, regression trees are prone to overfitting the data. To prevent
 275 overfitting, a variety of regularization techniques can be employed. This study minimizes the cost

276 complexity function, which places a penalty for each additional node that is selected for the model. As
277 shown below, the cost complexity function $R_\alpha(T)$ has two terms that influence its value:

278
$$R_\alpha(T) = R(T) + \alpha * f(T), \quad \text{Eq. 7}$$

279 where $R(T)$ is the training error, $f(T)$ is the number of leaves in the regression tree, and α is the
280 regularization parameter that is determined via cross-validation [41]. In Section 2.3 the cross-validation
281 procedure used in this study is thoroughly discussed.

282 Regression trees have the advantage that they do not assume linearity in the data, and, therefore, no
283 complex data transformations are needed. Overall, this approach is simpler than linear methods, but it
284 requires careful consideration so as not to overfit the data. Regression trees also implicitly select
285 variables, which means that a trained regression tree will show variables that have more importance for
286 predicting the target variable in earlier nodes in the tree. Lastly, regression trees are interpretable and can
287 provide some insight on the dataset being analyzed.

288 A disadvantage of simple regression trees is that they suffer from model instability; in other words,
289 small changes to the dataset might create a completely different set of partitions, and, consequently does
290 not lead to the best-performing model. For this reason, more complicated tree-based methods are often
291 considered that are more stable. Random forest and boosted trees are examples of more complex tree-
292 based methods that aim to reduce this instability and are discussed in the subsequent sections.

293 **2.1.5 Random Forest**

294 Random forest is a method that builds an ensemble of regression trees in order to reduce the instability of
295 individual trees. Random forest utilizes two strategies for improving the instability issue. First, it employs
296 the concept of “bootstrap aggregation” (sampling with replacement) in order to generate many similar
297 datasets that were sampled from the same original dataset. These datasets each lead to an individual tree
298 within the ensemble. Second, it incorporates randomness during tree-learning in order to reduce the
299 correlation between each tree within the ensemble. For instance, when generating new nodes (for
300 individual trees within the random forest), only a subset of the original predictor variables is selected as
301 the set of candidate variables on which to partition the data. The variable value that minimizes variance in
302 the output from these randomly selected predictors is the variable selected for that node. This process is
303 repeated for all nodes in a regression tree and then for all regression trees in the random forest. For a
304 random forest model, the tuning parameters are: the number of randomly selected predictors (k), the
305 number of individual trees that are trained (n), and the tree depth (d) [42].

306 The advantage of the random forest method is that it significantly reduces the instability of simple
307 regression trees. Furthermore, this method has been shown to minimize correlation between trees
308 compared to other tree-ensemble methods (e.g. “bagging trees” that use only bootstrap aggregation and

309 not random variable selection) [40]. One disadvantage of random forests is their reduction in
310 interpretability compared to simple regression trees; random forests cannot be easily visualized and
311 individual trees are often not good predictive models on their own. However, variable importance plots
312 can reveal the relative importance of predictor variables.

313 **2.1.6 Boosted Trees**

314 Like random forest, boosted trees are an ensemble method for dealing with the instability and poor
315 predictive performance of simple regression trees. Generally, the concept of “boosting” is an ensemble
316 strategy that can be used to improve weak learning algorithms (e.g. regression trees) [43], [44]. Boosting
317 can be applied to any weak learning algorithm but is commonly utilized for regression trees. The main
318 concept of boosting is to build a model using the weak learning algorithm. Then another model is learned
319 on the *residuals* from the first model. This step of model-building on the previous model’s residuals is
320 repeated for a set number of iterations. Therefore, a boosted tree is simply a model where the weak
321 learning algorithm used in each iteration is a regression tree.

322 Unlike random forest in which all trees are of the same importance, boosted trees are hierarchical,
323 meaning that each tree layer is constructed recursively. The tuning parameters for boosted trees are: the
324 number of trees, the interaction depth (maximum number of nodes per tree), the minimum number of
325 observations per node (a stopping criteria used to prevent trees that have only one observation at each
326 leaf), and the shrinkage rate (the rate at which the impact of each additional tree is reduced).

327 Boosted trees are similar to random forest in their advantages and disadvantages. Boosted trees tend to
328 have high predictive performance on highly nonlinear datasets and can be successful on problems where
329 there is unequal importance of predictor variables [34]. One disadvantage of boosted trees is that this
330 method has low interpretability; it is difficult to gain much intuition of the patterns that the model has
331 learned or to determine why a boosted tree model is successful (or not) at predicting the target variable.
332 This means that a strong ML pipeline must be used to train boosted trees to ensure that the approach has
333 not overfit the data.

334

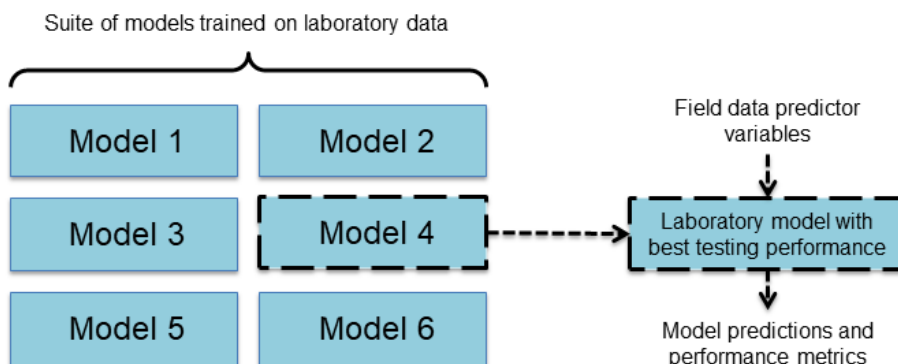
335 *2.2 Testing of Laboratory and Hybrid Models for Field Concrete Strength Prediction*

336 **2.2.1 Laboratory Models**

337 As was discussed in the introduction, many studies in the literature have developed ML models for
338 predicting concrete compressive strength using laboratory concrete datasets. While these laboratory
339 models report high predictive performance [2], [4]–[8], [10], [26], [27], it has not yet been tested whether
340 they are useful for predicting the compressive strength of field concrete. A significant novelty of this
341 study is that laboratory models are tested to determine if they are, in fact, useful for predicting
342 compressive strength when presented with other datasets – namely, field concrete data.

343 One issue preventing the direct testing of laboratory ML models from the literature is the use of
344 concrete age as a predictor variable. In other studies, age is a convenient predictor variable because it can
345 explain a high percentage of variance in compressive strength data. In other words, removing age as a
346 predictor and using only the final compressive strength as the output causes the compressive strength
347 problem to be significantly more difficult (*i.e.*, model performance measures tend to be poorer). In this
348 analysis, the desired model output is the final compressive strength (approximated by the 28-day strength)
349 of a concrete mixture as a function of only the quantities of the mixture ingredients. Due to this difference
350 between the prediction problem described herein and that of the literature, laboratory models for
351 predicting the 28-day compressive strength using laboratory concrete data have been trained specifically
352 for this study. Model utility is examined via the process described below and illustrated in Figure 2.

353 First, the aforementioned suite of ML models (*i.e.*, linear regression, polynomial regression, kernel
354 regression, tree-based models) is trained and tested using the laboratory data described in Section 3. The
355 model with the best testing performance is selected. Then, the predictor variables from the field data are
356 used as inputs and the performance measures and diagnostic plots for this new data shall be reported and
357 analyzed.



358

359 **Figure 2.** Process for testing the predictive capability of laboratory models using field concrete data. The
360 dotted outline indicates the laboratory model that is selected based on its performance measures.

361 **2.2.2 Models Trained on Hybrid Data**

362 It was hypothesized that the previously-described laboratory model will not satisfactorily predict the
363 compressive strength of real concrete mixtures. Thus, an analysis of models trained on hybrid data (*i.e.*, a
364 dataset that is composed of both field laboratory data) is conducted to determine whether they can
365 improve predictive performance compared to “pure” laboratory models.

366 Models trained on hybrid data are potentially valuable because there is an inherent tradeoff between
367 the use of laboratory and field models for predicting real concrete compressive strength. On one hand,
368 laboratory data is the cheapest and most accessible data to acquire. It is also the best method for exploring

369 new and exotic concrete mixtures that are uncommon in industry. However, laboratory compressive
370 strength data has the disadvantage that it does not reflect the full set environmental variables experienced
371 by field concrete. Accordingly, it is expected that ML models trained on hybrid data may have the
372 potential to improve the predictive performance of laboratory models.

373 In this novel hybrid approach, a percentage, α , of the hybrid dataset is composed of the field data, and
374 the rest is composed of the laboratory dataset. This procedure is used to determine if small amounts of
375 field data can improve model performance. In order to determine the effect of variable amounts of field
376 data, different α values are utilized (10%, 20%, 30%, 40%, and 50%). The model building process occurs,
377 as follows, for each value of α :

378 For each α :

- 379 1. Sort the field dataset in the order of lowest compressive strength to highest compressive strength
380 and partition this sorted dataset into quintiles.
- 381 2. In order to ensure the field data portion of the hybrid data is well-sampled, randomly sample (in
382 equal number) the appropriate number for points from the quintiles of the sorted field dataset.
383 Randomly sample from the field dataset the appropriate number of points.
- 384 3. Use this hybrid data to train a cross-validated ML model. (The selection of ML model is
385 determined by the best performing laboratory model.)
- 386 4. Use the remaining, unsampled field data to determine the average testing performance of the
387 hybrid model. The performance measures described in the following section are reported.
- 388 5. Repeat steps 1-4 five times to find average performance measures for each α .

389 *2.3 Performance Measures*

390 When training statistical, data-driven models, it is necessary to have a method to quantify the model
391 performance so that hyperparameter tuning can be iterated to select the best possible model. There are
392 several established metrics for determining predictive performance, each with advantages and
393 disadvantages, which will be discussed below. Common quantitative performance measures common to
394 regression modeling (rather than classification modeling) include the coefficient of determination (R^2),
395 root mean square error (RMSE), and mean absolute error (MAE) [45], [46]. These metrics, coupled with
396 model diagnostic plots and visualization of predicted versus observed output values, provide a
397 comprehensive picture of a model's performance.

398 R^2 is a measure of the proportion of the variance in the data that is explained by the model.
399 Accordingly, R^2 is the ratio shown in Eq. 8, where y_i is the observed value from the data, \hat{y}_i is the
400 predicted value from the model, and \bar{y} is the average output from the data.

$$401 R^2 = \frac{\sum_i (\hat{y}_i - \bar{y})^2}{\sum_i (y_i - \bar{y})^2} \quad \text{Eq. 8}$$

402 The value of R^2 ranges from zero to one, with higher values indicating a better ability to explain the
403 variance in the data with the model. However, R^2 is a measure of correlation, not accuracy, and should be
404 used with other performance measures because it is dependent on the variance of the output variable.

405 The root mean square error (RMSE) indicates how concentrated the data is around the model fit. The
406 RMSE is measured on the same scale as the output variable, and is always positive due to the squared
407 residuals in its calculation. Using the RMSE accentuates the effect of outliers in the error metric. This
408 means that if median error of the model (usually captured by the mean absolute error) is low, the RMSE
409 of the model can still be large due to the inability to model some outliers in the data. Given observed
410 values, y_i , predicted values, \hat{y}_i , and n observed values RMSE is calculated as:

$$411 \quad RMSE = \sqrt{\frac{\sum_{i=1}^n (\hat{y}_i - y_i)^2}{n}} \quad \text{Eq. 9}$$

412 The mean absolute error (MAE) is a measure of prediction accuracy of a model that uses the absolute
413 value of the errors rather than a squared value. The use of the absolute value reduces the influence of very
414 large errors on the measure of performance. Thus, MAE is a measure of the median error of the model
415 and is complimentary to the use of R^2 and RMSE.

$$416 \quad MAE = \frac{\sum_{i=1}^n |\hat{y}_i - y_i|}{n} \quad \text{Eq. 10}$$

417 Like RMSE, MAE is measured on the same scale as the output variable, and a lower value indicates a
418 better model fit. In addition, MAE values for a model are typically smaller than the RMSE value for the
419 same model. In this paper we chose to use both RMSE and MAE in order to report both the median and
420 mean error of each model.

421 2.4 Cross-validation

422 A critical issue to consider when training and comparing statistical and machine learning models is the
423 prevention of *overfitting*. Overfitting is a problem for ML models that have a high capacity to learn non-
424 linear relationships and are trained on datasets that do not contain a sufficiently large variance of the data
425 (*i.e.*, on datasets that are not rigorously sampled). When using iterative training methods such as grid
426 search, a model is particularly prone to overfitting if the same data is used for the training and validation
427 datasets. In this case, the resulting performance measures would indicate that the model has good
428 predictive performance, but when these models are tested on new data, poor performance is observed.

429 To prevent overfitting, ML learning methods and pipelines can employ several strategies. The strategy
430 employed herein, is called nested cross-validation (nested CV), which splits the data into “training”,
431 “validation”, and “testing” datasets. In the “inner CV loop”, the performance measures are approximately
432 optimized by fitting a model to each of several training datasets. Subsequently, the performance measures
433 are directly optimized by selecting hyperparameters with each validation dataset. In the “outer CV loop”,

434 the testing error is estimated by averaging test set scores for several dataset splits. In order to prevent data
435 leakage, it is critical that the trained models have never been exposed to the testing data.

436 When performing CV, the selection of the sizes of the training, validation, and testing sets is critical
437 because this choice affects the bias/variance tradeoff for a given statistical model. To strike a balance
438 between bias and variance error, this paper uses five folds (*i.e.*, partitions) for both the inner and outer CV
439 loops which can generate a favorable bias/variance tradeoff according to the literature [34]. This choice
440 results in 25 validation scores and 5 testing performance measure scores for each model.

441 **3. Datasets**

442 In this study, two datasets – field and laboratory concrete compressive strength data - are used. The field
443 dataset is from the Colorado Department of Transportation (CDOT); it has 1681 mixture designs and
444 corresponding compressive strength values. The mixture constituent variables in this dataset include
445 masses of cement, fly ash, water, water-reducing admixtures (WRA), coarse aggregate, fine aggregate,
446 and percent air entrainment. The laboratory dataset was obtained from the Machine Learning Repository
447 at the University of California, Irvine [35]. This dataset contains over 1000 mixture designs and
448 corresponding compressive strength values. However, it originally contained some mixtures that included
449 blast-furnace slag (a mixture ingredient not included in the field dataset) as well as some mixtures in
450 which the compressive strength was measured earlier than 28 days of curing. In order to reconcile these
451 differences, only mixtures that do not include blast furnace slag and that measure compressive strength
452 after 28 days are included in this analysis. This decision reduced the number of usable mixtures to 311.
453 One last discrepancy is that the laboratory dataset does not report air entrainment values. It is not clear
454 which of the following is true: a constant amount of air was entrained, no air was entrained, or variable
455 amounts of air were entrained but not reported. Notably, this discrepancy does not prevent model training
456 for either dataset. However, when the best laboratory predictive model is used to predict field
457 compressive strength, the air entrainment predictor cannot be utilized.

458

459 Table 1 provides a statistical summary of the two datasets. The laboratory dataset has been converted
460 to US customary units for ease of comparison. Note also that both datasets have used the Absolute
461 Volume Method for proportioning concrete mixtures, which generates weights of ingredients on a cubic
462 yard basis; this means that ingredient quantities are comparable between datasets.

463

464 **Table 1.** Statistical summary of laboratory- and field-acquired datasets.

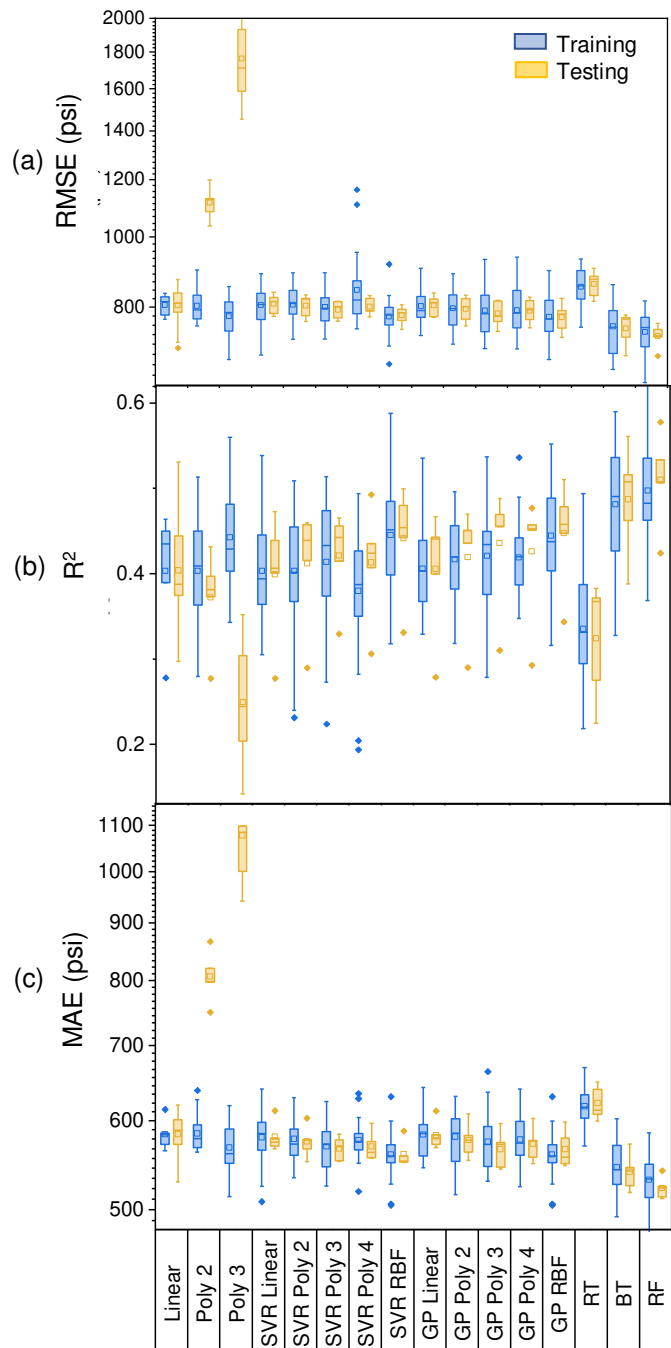
Dataset	Statistic	Cement	Fly Ash	Coarse Aggregate	Sand	Water	Air	WRA	Strength
	Units	lbs/yd ³	Vol. %	oz/yd ³	psi				
Lab	Mean	501	113	1678	1332	307	-	149	5357

	Median	487	161	1689	1330	314	-	154	5362
	Min	227	0	1350	1001	236	-	0	1239
	Max	910.2	337	1896	1593	384	-	761	11602
Field	Mean	540	106	1697	1256	265	6.6	28	5938
	Median	528	120	1725	1250	265	5.8	24	5820
	Min	395	0	430	445	142	0	0	3400
	Max	900	250	2240	2250	392	9.6	305	13040

465

466 **4. Results and Discussion**

467 In this analysis, we evaluate the predictive performance of the aforementioned ML models. The values for
 468 RMSE, MAE, and R^2 for all models are reported in Figure 3. Low values for RMSE and MAE, and high
 469 values for R^2 indicate better model performance, respectively. For simplicity of discussion, RMSE is used
 470 as the primary metric of performance. In addition, both the testing and validation performance is reported,
 471 which facilitates the discussion on overfitting in the models. These performance measures are plotted as
 472 boxplots to illustrate the range and variance of the error. The set of errors for each model is determined
 473 using a nested five-fold cross-validation, with five testing values and twenty-five training values for each
 474 model. Each model's performance from a methodological standpoint is discussed in the sections to
 475 follow. The methodological and architectural reasons for each model's performance are also examined.



476

477 **Figure 3.** Boxplots of the three cross-validated performance measures – (a) RMSE, (b) R^2 , and (c) MAE
 478 for all ML models. Both the training and testing performance measures are reported. The abbreviations
 479 are as follows: linear regression (Linear), polynomial regression (Poly), support vector regression (SVR),
 480 Gaussian process regression (GP), regression tree (RT), boosted tree (BT), random forest (RF). Kernels
 481 are referred to as follows: second-order polynomial (Poly 2), third-order polynomial (Poly 3), fourth-
 482 order polynomial (Poly 4), radial basis function (RBF).

483 *4.1 Linear Regression*

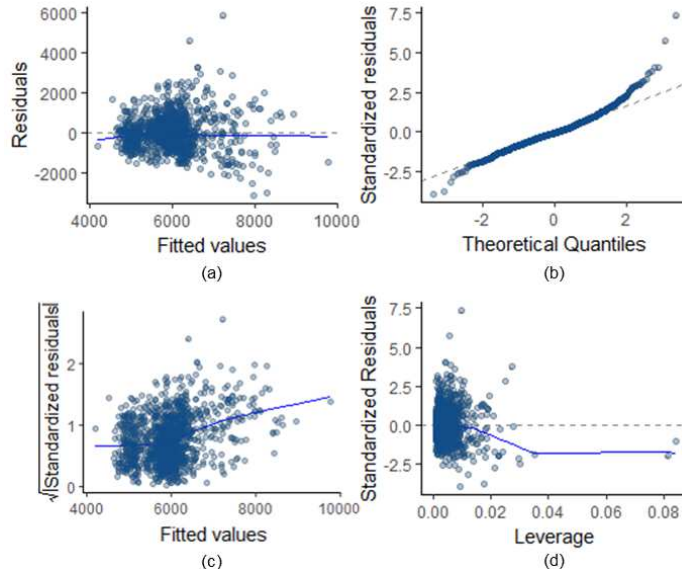
484 Linear regression is the first model tested in this analysis. This model assumes that the predictors are
485 independent and the residuals are homoscedastic and normally distributed. The performance of linear
486 regression is used as a baseline for comparing model performance and for determining what other models
487 may be more appropriate for the data. For the linear regression model, Bayesian information criterion
488 (BIC) – a parsimonious model selection criterion – is employed to select important predictor variables. Of
489 the seven mixture ingredients, BIC selects five of these as predictor variables (cement, fly ash, water, air,
490 and WRA); this model has a mean testing RMSE, MAE, and R^2 of 803 psi, 582 psi, and 0.40,
491 respectively. Of note is the relatively low value of R^2 , which indicates that a linear model is only able to
492 capture 40% of the variance in the data.

493 There are two possible reasons for the poor performance of this model. One reason is that there are
494 strong predictor variables that were not measured in the dataset. Consequently, the model does not have
495 all necessary information and is unable to perform well. A second possible reason is that the data does not
496 fit the linear assumption of the model, that is, the assumption that the predictors are linearly to produce an
497 output. These possibilities are further evaluated below in diagnostic plots.

498 Four diagnostic plots are shown in Figure 4. Figure 4a shows a plot of the residuals versus the
499 predicted outputs; significant deviation of the smoothed red line indicates non-constant error variances
500 and outliers. For this model, the smoothed average of the error variances indicates nearly constant error
501 variance. The quantile-quantile (Q-Q) plot (Figure 4b) diagnoses the normality of the residuals. Normal
502 residuals (in the statistical sense) lie along the dotted line; however, this figure indicates that there is some
503 deviation from normality of the residuals among higher residual values. Figure 4c is a scale-location plot,
504 which illustrates whether the homoscedasticity assumption is violated. For this plot, the residuals are
505 standardized (to have a mean of zero and a variance of one) and the absolute value is taken. This plot
506 shows that there is a slight increase in error variance with increasing compressive strength, which is
507 indicative of minor heteroscedasticity. Lastly, Figure 4d shows the standardized residuals against their
508 leverage, which is helpful for indicating if particular points more strongly influence the regression. In this
509 case, a few outlier points more highly influence the regression. However, the figure also plots contours of
510 the Cook's distance measure, which measures the effect of deleting a given observation. Cook's distance
511 is increased by both leverage and large residuals. Since no points have a Cook's distance greater than 0.5,
512 there is no great concern about large residuals also having too great of leverage over the fit.

513 One conclusion from the model diagnostics is that there are only minor assumption violations (non-
514 normality of residuals and heteroscedasticity). Despite this result, the linear model retains poor predictive
515 performance, which indicates that there are unmeasured variables needed for predicting compressive

516 strength. Nevertheless, it is reasonable to investigate the use of other types of models to determine if
517 improved performance can be achieved.



518

519 **Figure 4.** Model diagnostic plots: **(a)** Residuals versus predicted plot to check for non-constant error
520 variance for both positive and negative residuals, **(b)** Quantile-quantile plot to check normality of
521 residuals, **(c)** Scale-location plot to inspect homoscedasticity, and **(d)** Residuals versus leverage plot to
522 determine if any outliers severely impact the regression equation. The blue lines represent the smoothed
523 average for each model diagnostic.

524 **4.1.1 Polynomial Regression**

525 Polynomial regression introduces higher order terms and interaction terms between variables, which can
526 sometimes improve model performance because they approximate unobserved phenomena. Here, the
527 polynomial regression has potential because the linear regression analysis indicates a lack of the
528 necessary predictors for improving model performance. In this analysis, polynomial regression is
529 employed for second order and third order terms to determine if there is a physical basis for higher order
530 variables or interaction terms.

531 One key aspect of polynomial regression is that the method acts like a feature selection method. In
532 other words, a set of polynomial features is created, and then the features with the largest reduction in
533 RMSE are kept for the final model. This is the method by which interaction terms are discovered. During
534 the experiments in this paper, the following terms were discovered and included in the model:
535 $(Water) \times (WRA) \times (Air)$ and $(Cement)^2 \times (Fly\ ash)$. The first feature is somewhat intuitive; it is
536 expected that some interaction between water and WRA would be relevant. However, it is somewhat less
537 intuitive that air content is also a part of this feature. The second feature is intuitive because it is expected

538 that fly ash and cement would interactively have an impact on concrete compressive strength.
539 Promisingly, polynomials of order two and three decrease the *training* RMSE compared to the linear
540 model by 2.0% and 2.8%, respectively. Given this trend, it's likely that the RMSE of this model will
541 decrease given unlimited computational power.

542 However, it is critical to also analyze the testing error. The testing error values for polynomial orders
543 two and three are higher than the training error by 40.6% and 123.8%. This result suggests that the
544 polynomial regression models are too flexible and overfit the data as the polynomial order grows. Thus
545 this model type is not suitable for compressive strength prediction in concrete.

546 *4.2 Kernel Transformations and Regression*

547 A different approach to discovering interactions and modeling unobserved phenomena is to use non-linear
548 transformations of the data. Some of these are commonly known as kernel transformations. This section
549 will survey techniques in using kernel transformations.

550 **4.2.1 Support Vector Regression**

551 Solving the regression problem using kernel transformations, support vector regression is a popular
552 technique that has shown good results in the literature. In this paper, an array of kernels was tested in
553 cross-validation. These kernels include the RBF kernel, and polynomial kernels (2, 3, and 4).
554 One of the major goals of adaptive regression techniques like SVR is to discover any underlying structure
555 in the data. Of the tested kernels, the RBF kernel has the greatest reduction in RMSE compared to linear
556 regression. Here, RBF SVR reduces the average RMSE by 2.9%. In contrast, the linear and polynomial
557 kernels (orders 2, 3, and 4) reduce this error by -0.6%, -0.1%, 1.1%, and 0.2%, respectively.
558 From this result, it is inferred that the RBF kernel generates the optimal hyperplane for linearly separable
559 patterns among the tested kernels. The minimal improvement from polynomial kernels implies that the
560 regression curve is not well-modeled by a polynomial.

561 The performance of SVR with RBF demonstrates that transformation of the predictor variables
562 improves upon the linear regression baseline model. However, as will be demonstrated in section 3.3,
563 further improvements in performance can be made with other models. One possible explanation for this
564 behavior is that SVR can suffer from the curse of dimensionality in the sense that all terms in the
565 transformed space are given equal weight, so the kernel cannot adapt itself to focus on the critical
566 “subspaces” of the data [34]. Hastie et al. illustrates this concept via a prediction problem with four
567 standard normal features (*i.e.*, “real” features) with a polynomial decision boundary and six Gaussian
568 random features (*i.e.*, “noise” features) [34]. Although applying a polynomial kernel with SVR reduces
569 the test error, the real features are drowned out by the noise features. In the example, kernelized SVR is
570 unable to perform as well compared to when the real features are the only modeled features. We
571 hypothesize that this behavior is also true in this case; the noise of irrelevant variables essentially

572 overpowers the predictive capability of SVR to capture the true underlying behavior of field compressive
573 strength.

574 **4.2.2 Gaussian Process Regression**

575 As is displayed in Figure 3 the GP training and testing performance show that the RBF kernel also
576 generates the highest performance for GP for the kernels utilized in this study. Compared to the linear
577 regression baseline, the GP with RBF-transformed data decreases the average testing RMSE by 3.6%.
578 Utilizing the linear and polynomial (orders 2, 3, and 4) transformations, the reduction in RMSE is -0.1%,
579 1.0%, 2.5%, and 1.6% respectively. With these results, we can conclude that the same transformation
580 (RBF) generates the hyperplane most suitable for use in both SVR and GP.

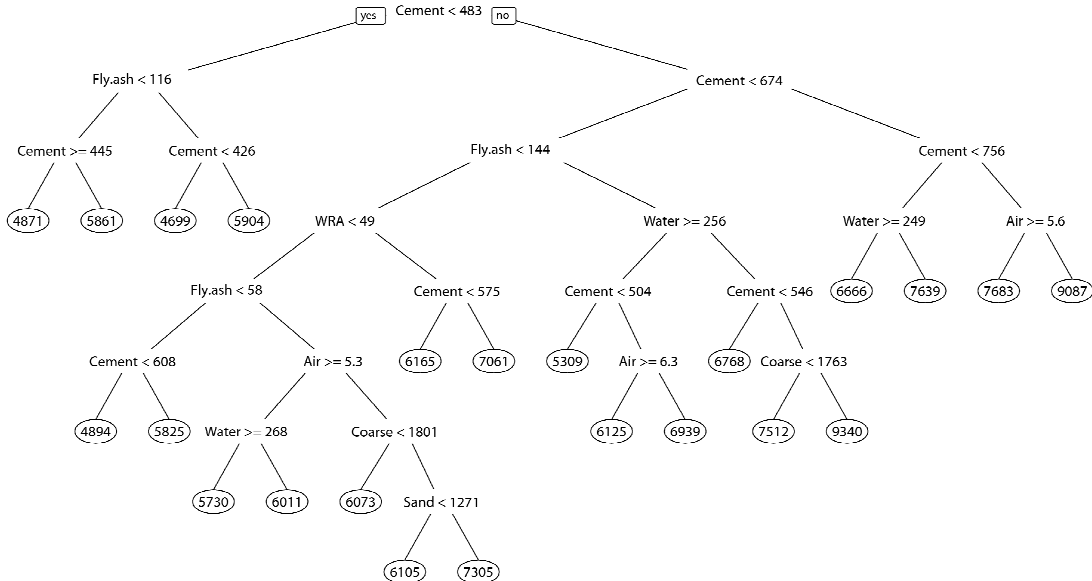
581 Moreover, this analysis shows that GP is preferred over SVR for this type of data due to its improved
582 performance measures. We hypothesize that GP is a better-performing method (compared to SVR) due its
583 further relaxation of the linearity assumption. Unlike GP, SVR retains the assumption that a
584 transformation of the predictor space causes the data to be linearly separable. GP, on the other hand,
585 makes predictions based on the maximum likelihood of an output given the data, normal parameter
586 distributions, and penalty term that minimize the prediction error. The improved performance of GP over
587 SVR indicates that model performance improves when no linearity assumption exists.

588 *4.3 Tree-based Models*

589 **4.3.1 Simple Regression Trees**

590 Unlike the aforementioned techniques, tree-based methods assume that the predictor variables may be
591 partitioned repeatedly and that each final partition generates a different output value. For the simplest
592 tree-based method (regression trees), the average testing RMSE indicates an increase of 6.9% compared
593 to linear regression. We hypothesize that this result is due to the instability of regression trees. In other
594 words, the constructed nodes for a tree may change significantly if the input training sample is slightly
595 changed. Figure 3 illustrates the decreased performance of this model for all three metrics: RMSE,
596 MAPE, and R^2 .

597 Although the testing performance of the simple regression tree indicates it should not be used for
598 prediction, the results of the model can be used to better understand the relative importance of certain
599 variables for determining concrete compressive strength. In Figure 7, the nodes (e.g. Cement < 569 lbs.)
600 and terminal node predictions (e.g. 4868 psi) are illustrated in the regression tree graph. Values of cement
601 are the first and second nodes, as well as multiple nodes lower in the tree, which indicate the importance
602 of cement quantity as a discriminating predictor variable for this tree. The next most important variable is
603 the quantity of fly ash, which, like cement, has positive correlation with strength. All of the mixture
604 ingredients appear in nodes in the tree, indicating that all are valuable for prediction.



605

606 **Figure 5.** This figure represents the best-performing simple regression tree graph for compressive
 607 strength prediction. Final predictions from each terminal node are shown in ellipses.

608 **4.3.2 Boosted Trees**

609 Boosted methods are used to reduce the instability of single trees. In this paper, the ensemble tree model
 610 reduced the average testing RMSE by 13.2% compared to the simple regression tree and by 6.9%
 611 compared to linear regression. For this dataset, boosted trees are the second best method for prediction
 612 based on the three performance measures. Notably, the average training RMSE for boosted trees (749 psi)
 613 is slightly lower than that of the random forest model (751 psi). However, the random forest model has
 614 the lower testing RMSE by 5.4%. Despite the nested cross-validation routine, it appears that the boosted
 615 tree model is slightly overfitted due to the higher value of testing RMSE compared to the training RMSE.
 616 Recall from section 2.1.6, that this method iteratively builds regression trees on the residuals from each
 617 consecutive tree. We hypothesize that the model has learned noise in the residuals rather than signal in the
 618 data, which has lead to lower testing performance.

619 **4.3.3 Random Forest**

620 Like boosted trees, the random forest model reduces the instability of simple regression trees by utilizing
 621 an ensemble of trees that utilize bootstrap aggregation and random variable selection. Consequently, the
 622 model decreases the average testing RMSE by 9.4% compared to the linear model. It also improves upon
 623 the testing RMSE of the simple regression tree by 20.0%. Furthermore, the average testing error is
 624 slightly lower than the average validation error (730 psi versus 739 psi) indicating that it is unlikely that

625 the random forest model is overfitted. These testing and validation performance measures indicate that
626 random forest is the best method for predicting compressive strength with this dataset. It has the lowest
627 RMSE and MAE as well as the highest R² value (730 psi, 530 psi, and .51, respectively).

628 This result may be due to the ability of tree-based methods to learn inconsistent variable importance in
629 the data. In other words, each tree, trained on a subset of the data might learn a slightly different set of
630 variable importance weights. In aggregate, the random forest can then better predict the target variable.
631 An example of inconsistent variable importance can be seen in Figure 5; for mixtures with cement
632 quantities of less than 569 pounds, the next most important variable for determining strength is fly ash. In
633 contrast, above 569 pounds, the next splitting criterion is an even higher quantity of cement. Not only do
634 random forest models have the ability to learn inconsistent variable importance, they also reduce the
635 instability of individual trees and reduce the potential for overfitting [47].

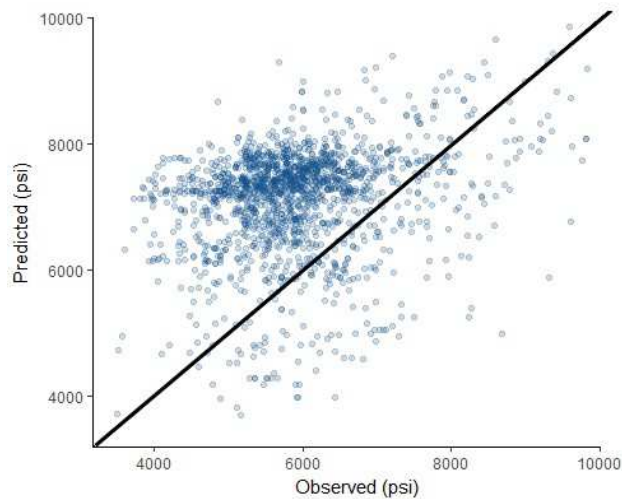
636 *4.4 Prediction of Field Compressive Strength with Laboratory and Hybrid Models*

637 **4.4.1 Models Trained on Laboratory Data**

638 As was discussed in Section 2, many studies in the literature have developed ML models for predicting
639 concrete compressive strength using laboratory datasets. While these laboratory models report high
640 predictive performance, it is relevant to consider whether they are useful for predicting field concrete
641 strength.

642 Consequently, in this study, a suite of ML models (*i.e.*, linear regression, polynomial regression,
643 kernel regression, tree-based models) is trained and tested using the laboratory data described in Section
644 3. Among those tested, the highest-performing model for the laboratory dataset is the random forest
645 model, in which the number of random variables selected at each node was 3, and the number of trees was
646 550 trees; this model achieves a testing R² value of 0.80.

647 Subsequent to the random forest model selection, the predictor variables from the field data have been
648 used as inputs in the laboratory random forest model to determine how well the model can predict
649 compressive strength of real concrete. The predicted output is plotted versus the observed field strength
650 value in Figure 6. Points near the 1:1 line would indicate a high-performing model. This plot shows that
651 despite its high performance using laboratory data, the laboratory model is not able to predict field
652 strength to a high degree of accuracy; the RMSE for the field data is 1655 psi. Furthermore, this plot
653 illustrates that, overall, the laboratory model tends to over-predict compressive strength. It is likely that
654 this effect is due to the ideal curing conditions in the laboratory setting, which would tend to generate
655 higher compressive strength values than if the same mixture was cured under highly variable
656 environmental conditions.



657

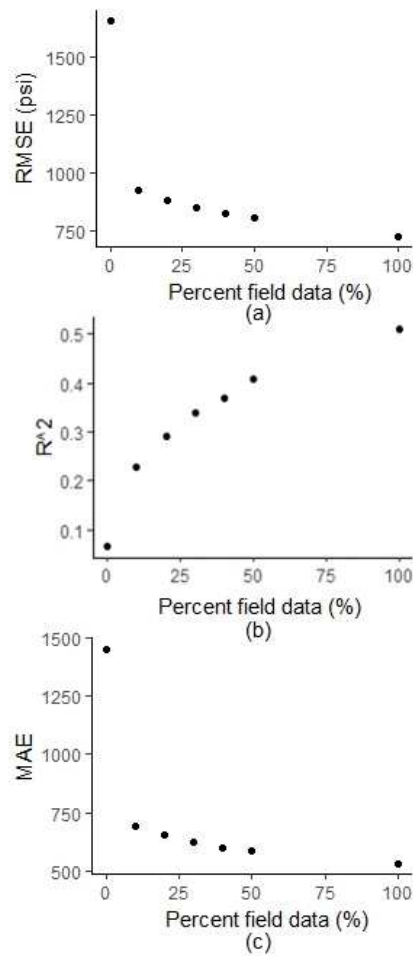
658 **Figure 6.** Predicted versus observed plot for field compressive strength predictions using the random
659 forest laboratory model, which illustrates the models tendency to overpredict strength.

660 **4.4.2 Models Trained on Hybrid Data**

661 As was described in Section 2.3.2, models employing hybrid training data are explored in order to
662 determine if small amounts of field data can improve the performance of laboratory ML models for
663 predicting compressive strength of field concrete. In this analysis, α values of 10%, 20%, 30%, 40%, and
664 50% replacement percentages are selected via the quintile sampling method discussed in section 2.3.2.
665 The remaining, unused field data is to determine the average testing performance of each hybrid model.

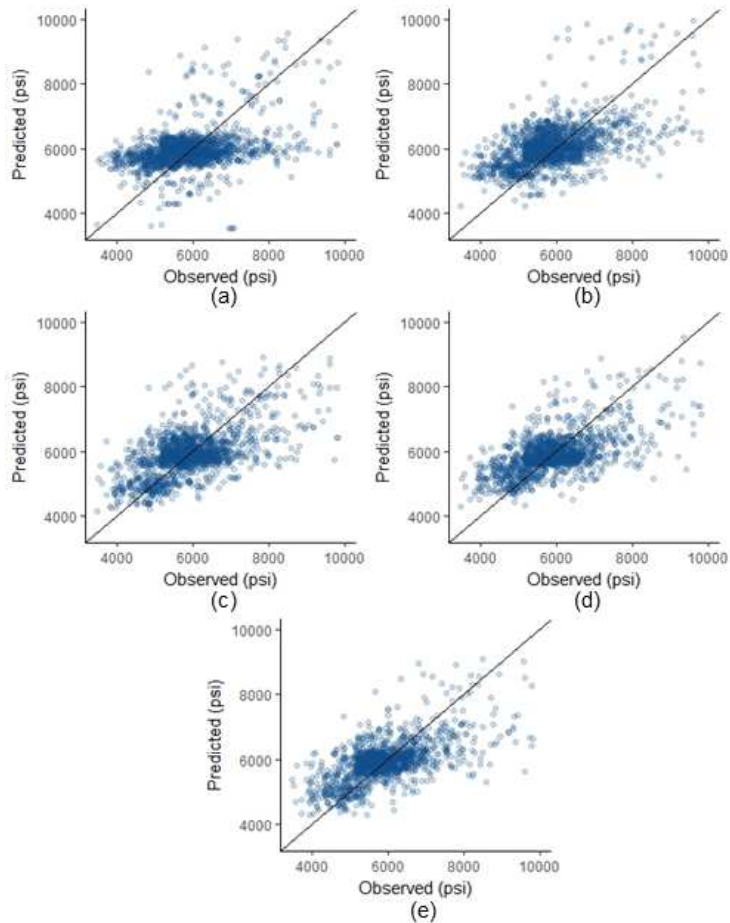
666 As was hypothesized, the inclusion of small percentages of field data significantly reduces the RMSE
667 MAE and increases the R^2 (compared to a pure laboratory model). As is shown in Figure 7, the most
668 significant model improvements occur with the addition of the initial 10% of field data, which reduces the
669 RMSE by 43.0%. However, continued performance improvements occur with the additional
670 supplementation of field data driving the models. Furthermore, Figure 8 illustrates via predicted vs.
671 observed scatter plots how the addition of field data improves predictive performance. A model
672 comprised of 100% field data, which was analyzed in Section 4.3, is the standard with which the hybrid
673 models are compared in terms of the extent to which predictive performance could be improved. This
674 analysis illustrates that ML modeling of hybrid training data is a promising area of research that improves
675 upon the downsides of field models and laboratory models being used in isolation.

676 Future research in this area may explore different ML methods (*i.e.*, models other than random forest)
677 or other hybridization strategies for utilizing hybrid training data. In addition, it may be of interest to
678 focus this modeling procedure on concretes with exotic mixture ingredients, which inherently have been
679 rarely employed in industry, and thus, have few data points with which to model compressive strength.
680



681

682 **Figure 7.** Graphs illustrating the continued improvement in (a) RMSE, (b) R^2 , and (c) MAE as additional
 683 field data is supplied to the model.



684

685 **Figure 8.** Scatter plots of predictive versus observed for ML models trained on hybrid data with the
 686 following percentages of field data: **(a)** 10%, **(b)** 20%, **(c)** 30%, **(d)** 40%, **(e)** 50%. Points lying near the
 687 one-to-one line indicate better model performance.

688 **5. Conclusions**

689 The goal of this work was to specifically analyze the compressive strength behavior of *field concrete* as a
 690 function of mixture ingredient quantities. Furthermore, this work trained and tested a variety of ML
 691 models for predicting compressive strength of field concrete mixtures and determined which ML models
 692 are best suited for the data. By analyzing the performance measures and a variety of diagnostic plots, the
 693 reasons for differing performance for field concrete ML models have been elucidated. For instance, from
 694 the linear regression model diagnostics, it was found that there are only very minor violations of linearity
 695 assumptions; this result indicated it is likely that important predictor variables are missing from the data.
 696 Further manipulation of the predictor space via polynomial regression and kernel transformation indicated
 697 that a transformed predictor space can improve predictive capability (via a 4% reduction in testing
 698 RMSE). Moreover, it was found that nonlinear models, specifically random forest, generated the best

699 performance measures, which is attributed to its full rejection of linear assumptions and ability to learn
700 inconsistent variable importance in the data.

701 It was also confirmed that, at the current time, the most accurate prediction of compressive strength of
702 field concrete is achieved with models trained on field concrete data; however, ML models that employ
703 hybrid training data show promise for significantly improving predictive performance of laboratory
704 concrete models even when only small amounts of field concrete data are available. For instance, it was
705 found that, when only 10% of the training data were from field concrete, the RMSE was reduced by 43%.
706 Moving forward, this research could be extended to explore other ML models with the hybridized
707 approach or applications when it is desirable to explore modeling of exotic concrete mixtures and
708 ingredients.

709 Broadly, the results of this research support two main conclusions: (1) Prediction of field concrete
710 strength requires the application of nonlinear ML models using field-specific data. In particular, advanced
711 tree-based models, such as random forest, are the highest-performing, even when field data is relatively
712 less abundant than laboratory data. (2) Although there is value in testing and statistical-model training for
713 the strength prediction of laboratory concrete, these models should not be used for stand-alone prediction
714 of field concrete strength, because they do not capture the many convoluting factors of field concrete
715 placement and curing. However, ML models that employ hybrid training data can significantly improve
716 the predictive performance compared to laboratory concrete ML models that are used in isolation.

717

718 **6. Acknowledgments**

719 This research was made possible by the Department of Civil, Environmental, and Architectural
720 Engineering, the College of Engineering and Applied Sciences, and the Living Materials Laboratory at
721 the University of Colorado Boulder, with support from the National Science Foundation (Award No.
722 CMMI-1562557). This work represents the views of the authors and not necessarily those of the sponsors.

723

724 **References**

725 [1] ACI Committee 318, “Building code requirements for reinforced concrete,” American Concrete
726 Institute, ACI 318, 2014.

727 [2] M. Alshihri, A. Azmy, and M. El-Bisy, “Neural networks for predicting compressive strength of
728 structural light weight concrete,” *Constr. Build. Mater.*, vol. 23, no. 6, pp. 2214–2219, 2009.

729 [3] A. Oztas, M. Pala, E. Ozbay, E. Kanca, N. Caglar, and M. A. Bhatti, “Predicting the compressive
730 strength and slump of high strength concrete using neural network,” *Constr. Build. Mater.*, vol. 20,
731 no. 9, pp. 769–775, 2006.

732 [4] C. Bilim, C. D. Atış, H. Tanyildizi, and O. Karahan, "Predicting the compressive strength of ground
733 granulated blast furnace slag concrete using artificial neural network," *Adv. Eng. Softw.*, vol. 40, no.
734 5, pp. 334–340, May 2009.

735 [5] H.-G. Ni and J.-Z. Wang, "Prediction of compressive strength of concrete by neural networks,"
736 *Cem. Concr. Res.*, vol. 30, no. 8, pp. 1245–1250, Aug. 2000.

737 [6] J. Zhang and Y. Zhao, "Prediction of Compressive Strength of Ultra-High Performance Concrete
738 (UHPC) Containing Supplementary Cementitious Materials," in *2017 International Conference on*
739 *Smart Grid and Electrical Automation (ICSGEA)*, 2017, pp. 522–525.

740 [7] S.-C. Lee, "Prediction of concrete strength using artificial neural networks," *Eng. Struct.*, vol. 25,
741 no. 7, pp. 849–857, Jun. 2003.

742 [8] S. Akkurt, S. Ozdemir, G. Tayfur, and B. Akyol, "The use of GA-ANNs in the modelling of
743 compressive strength of cement mortar," *Cem. Concr. Res.*, vol. 33, no. 7, pp. 973–979, Jul. 2003.

744 [9] I. B. Topcu, "Prediction of properties of waste AAC aggregate concrete using artificial neural
745 network," *Comput. Mater. Sci.*, vol. 41, no. 1, pp. 117–125, 2007.

746 [10] U. Atici, "Prediction of the strength of mineral admixture concrete using multivariable regression
747 analysis and an artificial neural network," *Expert Syst. Appl.*, vol. 38, no. 8, pp. 9609–9618, Aug.
748 2011.

749 [11] M. Rguig and M. El Aroussi, "High-Performance Concrete Compressive Strength Prediction Bsed
750 Weighted Support Vector Machines," *Int. J. Eng. Res. Appl.*, vol. 7, no. 1, pp. 68–75, Jan. 2017.

751 [12] B. G. Aiyer, D. Kim, N. Karingattikkal, P. Samui, and P. R. Rao, "Prediction of compressive
752 stregnth of self-compacting concrete using least square support vector machine and relevance vector
753 machine," *KSCE J. Civ. Eng.*, vol. 18, no. 6, pp. 1753–1758, 2014.

754 [13] C. Deepa, K. Sathiya Kumari, and V. Pream Sudha, "Prediction of the compressive strength of high
755 performance concrete mix using tree based modeling," *Int. J. Comput. Appl.*, vol. 6, no. 5, pp. 18–
756 24, 2010.

757 [14] D. A. Abrams, "Water-Cement Ratio as a Basis of Concrete Quality," *J. Proc.*, vol. 23, no. 2, pp.
758 452–457, Feb. 1927.

759 [15] S. Popovics, "Analysis of Concrete Strength Versus Water-Cement Ratio Relationship," *Mater. J.*,
760 vol. 87, no. 5, pp. 517–529, Sep. 1990.

761 [16] M. S. Mamlouk and J. P. Zaniewski, *Materials for Civil and Construction Engineers*, 2nd ed. Upper
762 Saddle River, NJ: Pearson Education, Inc., 2006.

763 [17] R. Kozul, "Effects of Aggregate Type, Size, and Content on Concrete Strength and Fracture
764 Energy," University of Kansas Center for Research, Inc., Lawrence, KS, SM Report No. 43, 1997.

765 [18] A. Fernández-Jiménez and A. Palomo, “Characterisation of fly ashes. Potential reactivity as alkaline
766 cements☆,” *Fuel*, vol. 82, no. 18, pp. 2259–2265, Dec. 2003.

767 [19] A. A. Ramezanianpour and V. M. Malhotra, “Effect of curing on the compressive strength,
768 resistance to chloride-ion penetration and porosity of concretes incorporating slag, fly ash or silica
769 fume,” *Cem. Concr. Compos.*, vol. 17, no. 2, pp. 125–133, Jan. 1995.

770 [20] J. Fox, “Fly Ash Classification - Old and New Ideas,” presented at the 2017 World of Coal Ash
771 Conference, Lexington, KY, 2017.

772 [21] A. M. Zeyad, “Effect of curing methods in hot weather on the properties of high-strength
773 concretes,” *J. King Saud Univ. - Eng. Sci.*, May 2017.

774 [22] O. Cebeci, “Strength of concrete in warm and dry environment,” *Mater. Struct.*, pp. 270–272, 1987.

775 [23] B. A. Young, A. Hall, L. Pilon, P. Gupta, and G. Sant, “Can the compressive strength of concrete be
776 estimated from knowledge of the mixture proportions?: New insights from statistical analysis and
777 machine learning methods,” *Cem. Concr. Res.*, Sep. 2018.

778 [24] M. A. DeRousseau, J. R. Kasprzyk, and W. V. Srubar, “Computational design optimization of
779 concrete mixtures: A review,” *Cem. Concr. Res.*, vol. 109, pp. 42–53, Jul. 2018.

780 [25] I.-C. Yeh, “Optimization of Concrete Mix Proportioning Using Flattened Simplex-Centroid Mixture
781 Design and Neural Networks,” *Eng. Comput.*, vol. 25, no. 179, pp. 179–190, 2009.

782 [26] M. Pala, E. Özbay, A. Öztaş, and M. I. Yuce, “Appraisal of long-term effects of fly ash and silica
783 fume on compressive strength of concrete by neural networks,” *Constr. Build. Mater.*, vol. 21, no. 2,
784 pp. 384–394, Feb. 2007.

785 [27] G. Trtnik, F. Kavčič, and G. Turk, “Prediction of concrete strength using ultrasonic pulse velocity
786 and artificial neural networks,” *Ultrasonics*, vol. 49, no. 1, pp. 53–60, Jan. 2009.

787 [28] İ. B. Topçu and M. Sarıdemir, “Prediction of compressive strength of concrete containing fly ash
788 using artificial neural networks and fuzzy logic,” *Comput. Mater. Sci.*, vol. 41, no. 3, pp. 305–311,
789 Jan. 2008.

790 [29] Y. Ayaz, A. F. Kocamaz, and M. B. Karakoc, “Modeling of compressive strength and UPV of high-
791 volume mineral-admixed concrete using rule-based M5 rule and treemodel M5P classifiers,”
792 *Constr. Build. Mater.*, vol. 94, pp. 235–240, 2015.

793 [30] C. Videla and C. Gaedicke, “Modeling Portland Blast-Furnace Slag Cement High-Performance
794 Concrete,” *Mater. J.*, vol. 101, no. 5, pp. 365–375, Sep. 2004.

795 [31] F. Khademi, S. M. Jamal, N. Deshpande, and S. Londhe, “Predicting strength of recycled aggregate
796 concrete using Artificial Neural Network, Adaptive Neuro-Fuzzy Inference System and Multiple
797 Linear Regression,” *Int. J. Sustain. Built Environ.*, vol. 5, no. 2, pp. 355–369, Dec. 2016.

798 [32] M. Saridemir, “Prediction of compressive strength of concretes containing metakaolin and silica
799 fume by artificial neural networks,” *Adv. Eng. Softw.*, vol. 40, no. 5, pp. 350–355, May 2009.

800 [33] E. Güneyisi, M. Gesoğlu, Z. Algın, and K. Mermerdaş, “Optimization of concrete mixture with
801 hybrid blends of metakaolin and fly ash using response surface method,” *Compos. Part B Eng.*, vol.
802 60, pp. 707–715, Apr. 2014.

803 [34] T. Hastie, R. Tibshirani, and J. Friedman, *The Elements of Statistical Learning: Data Mining,
804 Inference, and Prediction, Second Edition*, 2nd ed. New York: Springer-Verlag, 2009.

805 [35] “UCI Machine Learning Repository: Concrete Compressive Strength Data Set.” [Online].
806 Available: <https://archive.ics.uci.edu/ml/datasets/Concrete+Compressive+Strength>. [Accessed: 19-
807 Dec-2017].

808 [36] “R: The R Project for Statistical Computing.” [Online]. Available: <https://www.r-project.org/>.
809 [Accessed: 06-Nov-2018].

810 [37] G. A. F. Seber and A. J. Lee, *Linear Regression Analysis*. John Wiley & Sons, 2012.

811 [38] T. Hofmann, B. Scholkopf, and A. Smola, “Kernel Methods in Machine Learning,” *Ann. Stat.*

812 [39] H. Drucker, C. J. Burges, L. Kaufman, A. J. Smola, and V. N. Vapnik, “Support Vector Regression
813 Machines,” *Adv. Neural Inf. Process. Syst.* 9, pp. 155–161.

814 [40] C. Strobl, J. Malley, and G. Tutz, “An introduction to recursive partitioning: rationale, application,
815 and characteristics of classification and regression trees, bagging, and random forests,” *Psychol.
816 Methods*, vol. 14, no. 4, pp. 323–348, Dec. 2009.

817 [41] L. Breiman, *Classification and Regression Trees*. Routledge, 2017.

818 [42] P. Probst, M. Wright, and A.-L. Boulesteix, “Hyperparameters and Tuning Strategies for Random
819 Forest,” *ArXiv180403515 Cs Stat*, Apr. 2018.

820 [43] J. Friedman, T. Hastie, and R. Tibshirani, “Additive logistic regression: a statistical view of
821 boosting (With discussion and a rejoinder by the authors),” *Ann. Stat.*, vol. 28, no. 2, pp. 337–407,
822 Apr. 2000.

823 [44] J. H. Friedman, “Greedy function approximation: A gradient boosting machine.,” *Ann. Stat.*, vol. 29,
824 no. 5, pp. 1189–1232, 200110.

825 [45] T. Chai and R. R. Draxler, “Root mean square error (RMSE) or mean absolute error (MAE)? –
826 Arguments against avoiding RMSE in the literature,” *Geosci. Model Dev.*, vol. 7, no. 3, pp. 1247–
827 1250, Jun. 2014.

828 [46] P. N. Chatur, A. R. Khobragade, and D. S. Asudani, “Effectiveness evaluation of regression models
829 for predictive data-mining,” *Int. J. Manag. IT Eng.*, vol. 3, no. 3, pp. 465–483, Oct. 2013.

830 [47] L. Breiman, “Random Forests - Random Features,” University of California, Berkeley, CA,
831 Technical Report 567, Sep. 1999.